

Silent Very Late Thrombotic Occlusion of Sirolimus-Eluting Stent Confirmed by Directional Coronary Atherectomy

Takashi Nakayama, MD; Yoshio Kobayashi, MD; Hiroyuki Takano, MD;
Nakabumi Kuroda, MD; Kenzo Hiroshima, MD*; Issei Komuro, MD

Stent thrombosis is defined as thrombotic occlusion of a stent resulting in acute coronary syndrome (ACS). However, all thrombotic occlusions of stents might not result in ACS. The present case report describes silent, very late thrombotic occlusion of a drug-eluting stent that was confirmed from specimens removed by directional coronary atherectomy. (*Circ J* 2009; 73: 1762–1764)

Key Words: Angioplasty; Coronary artery disease; Restenosis; Stent; Stent thrombosis

Late stent thrombosis after drug-eluting stent (DES) placement has emerged as a major concern.^{1–4} Stent thrombosis is defined as thrombotic occlusion of a stent resulting in acute coronary syndrome (ACS),^{5–7} but all thrombotic occlusions of stents might not result in ACS. The present case report describes silent, very late thrombotic occlusion of DES that was confirmed from specimens removed by directional coronary atherectomy (DCA).^{8,9}

Case Report

A 61-year-old man with a history of hypertension was admitted because of exertional angina. Coronary angiography revealed 90% stenosis in the proximal left anterior descending coronary artery (LAD) and collaterals from the right coronary artery (**Figure 1A**), so the patient was referred for coronary angioplasty. An 18-mm sirolimus-eluting stent (SES, Cypher™, Cordis, Miami, FL, USA), premounted on a 3.5-mm balloon catheter, was deployed at 16 atm. The final angiogram (**Figure 1B**) and intravascular ultrasound (IVUS) (**Figure 2A**) showed a good result. He received ticlopidine (100 mg twice daily) plus aspirin (100 mg/day) for 3 months and thereafter was on aspirin monotherapy. Seven months later follow-up angiography demonstrated no in-stent restenosis (**Figure 1C**). Follow-up IVUS that was performed as part of clinical research demonstrated minimum intimal hyperplasia without incomplete apposition (**Figure 2B**).

Because of exertional angina persisting for several months, he was referred for coronary angiography 23 months after SES implantation. There were no electrocardiographic abnormalities to indicate ACS (**Figure 3**) or elevated levels of biomarkers for myocardial necrosis. Coronary angiography demonstrated total occlusion of the SES (**Figure 1D**) and complete filling of the LAD distal to the SES from the right coronary artery (**Figure 1E**). The patient was referred for coronary angioplasty. A 0.014-inch

Conquest Pro guidewire (Asahi Intecc, Seto, Japan) supported with a tornus catheter (Asahi Intecc) was crossed through the total occlusion. Predilatation using a 2.0-mm Lacrosse balloon catheter (Goodman, Nagoya, Japan) inflated at 6 atm was performed. The guidewire was then changed to a flexi-wire (Guidant, Santa Clara, CA, USA). IVUS was performed and demonstrated a heterogeneous mass in the stent (**Figure 2C**). With the informed consent of the patient, DCA using a Flexicut directional atherectomy device (Guidant) was performed with the intention of obtaining tissue in the stent to clarify the mechanism of delayed total occlusion (**Figure 1F**)^{8,9}; informed consent for a case report was obtained later. A total of 7 cuts were performed, inflating the balloon up to 50 psi. A 28-mm SES premounted on a 3.0-mm balloon catheter was then deployed at 18 atm. The final angiogram showed a good result (**Figure 1G**). Pathological examination of the DCA specimens demonstrated organized thrombus rather than neointima (**Figure 4**).

Discussion

DES has dramatically reduced the incidence of in-stent restenosis,^{6,7} but a new problem of late stent thrombosis has appeared.^{1–4} Previous clinical studies used relatively restrictive and non-uniform definitions of stent thrombosis.^{6,7} These definitions uniformly regarded evidence of any myocardial infarction with angiographic confirmation of in-stent thrombus or unexplained death within 30 days after the procedure as stent thrombosis, but varied when myocardial infarction was present without angiographic confirmation of target-vessel involvement. Thus, standardized definitions of stent thrombosis were required and were recently proposed by the newly formed Academic Research Consortium (ARC).⁵ Their definition of definite stent thrombosis requires the presence of ACS with angiographic or autopsy evidence of thrombus or occlusion. Probable

(Received March 25, 2008; revised manuscript received September 11, 2008; accepted September 16, 2008; released online January 14, 2009)
Department of Cardiovascular Science and Medicine, *Department of Diagnostic Pathology, Chiba University Graduate School of Medicine, Chiba, Japan

Grant: none.

Mailing address: Yoshio Kobayashi, MD, Department of Cardiovascular Science and Medicine, Chiba University Graduate School of Medicine, 1-8-1 Inohana, Chuo-ku, Chiba 260-8670, Japan. E-mail: yoshio.kobayashi@wonder.ocn.ne.jp

All rights are reserved to the Japanese Circulation Society. For permissions, please e-mail: cj@j-circ.or.jp

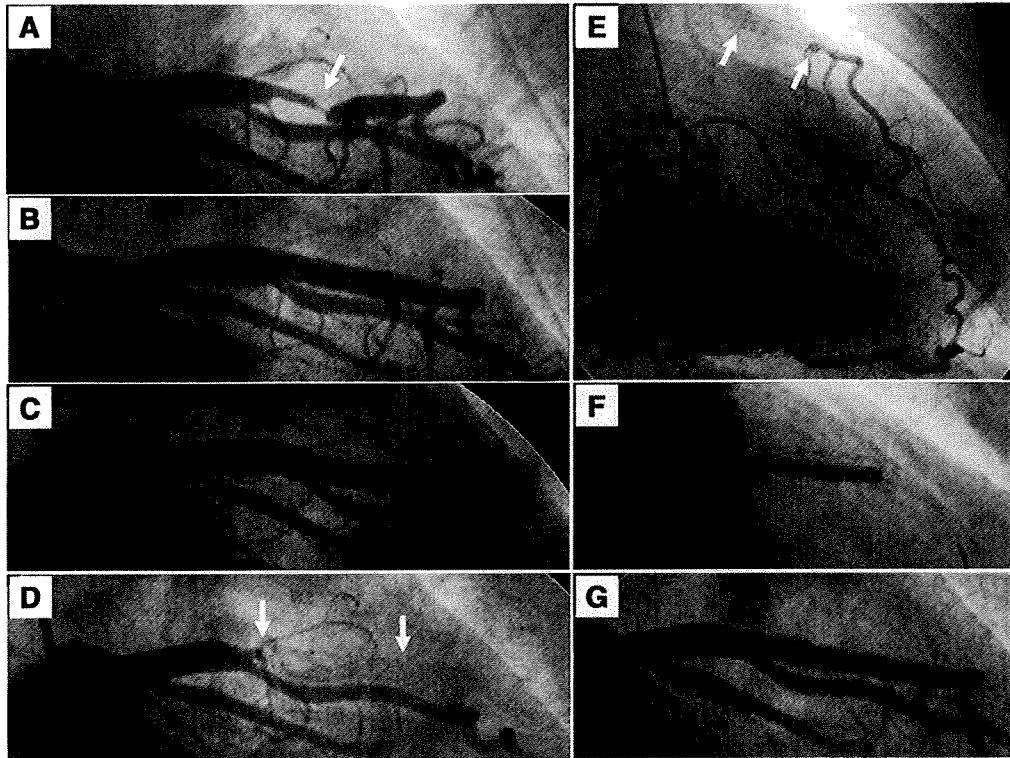


Figure 1. Coronary angiography showing 90% stenosis (arrow) of the proximal left anterior descending coronary artery (LAD) (A). After sirolimus-eluting stent (SES) implantation, angiography demonstrates a good result (B). Seven months later, follow-up angiography shows no in-stent restenosis (C). Coronary angiography demonstrates total occlusion of the SES (D) and complete filling of the LAD distal to the SES from the right coronary artery (E). Arrows (D,E) indicate the proximal and distal edges of the SES. Directional coronary atherectomy is performed (F) and the final angiogram shows a good result (G).

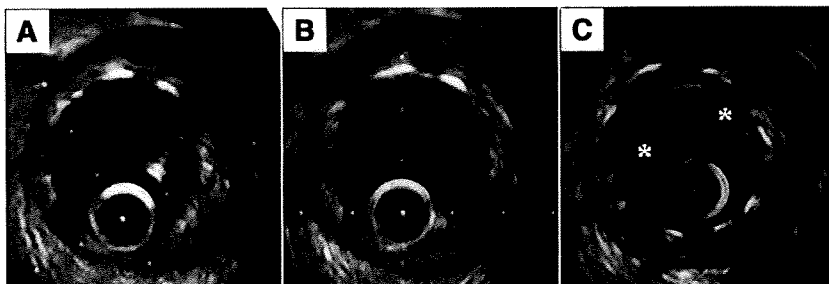


Figure 2. (A) Intravascular ultrasound (IVUS) after sirolimus-eluting stent implantation (stent cross-sectional area 7.6 mm^2). (B) Follow-up IVUS (stent cross-sectional area 7.7 mm^2). Note minimum intimal hyperplasia without incomplete apposition. (C) IVUS after predilatation for total occlusion (lumen cross-sectional area 2.6 mm^2 and stent cross-sectional area 7.7 mm^2). *Note heterogeneous mass in the stent.

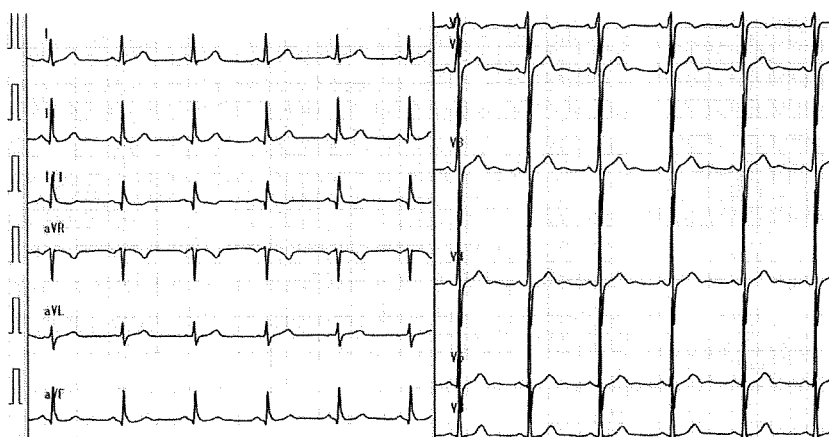


Figure 3. Electrocardiogram at 23 months after sirolimus-eluting stent implantation.

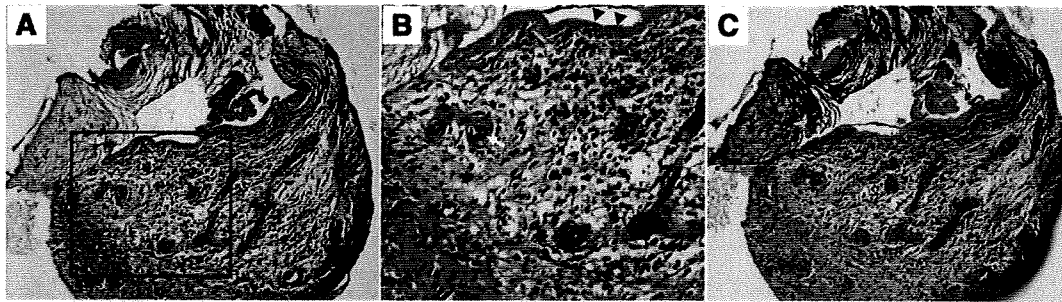


Figure 4. Hematoxylin and eosin (HE)-stained (A, B) and elastica van Gieson-stained (C) sections of a directional coronary atherectomy (DCA) specimen. (B) is a magnified view of the inset in (A). HE demonstrates fibrin (arrowheads), lymphocytes, fibroblast, hemosiderin-laden macrophages (black arrow) and neovascularization (white arrow). There are no smooth muscle cells and scant collagen fibers (red in C), which indicate that the DCA specimen is organized thrombus rather than neointima.

stent thrombosis includes unexplained death within 30 days after the procedure or acute myocardial infarction involving the target-vessel territory without angiographic confirmation. Possible stent thrombosis includes any unexplained death occurring at least 30 days after the procedure. Stent thrombosis was also classified as early (0–30 days), late (31–360 days) and very late (>360 days).

The reported incidence of late and very late stent thrombosis after DES implantation ranges between 0.2% and 0.7%.^{1–3} In the present case, very late thrombotic occlusion of SES occurred in a patient without ACS, which might be considered as delayed in-stent restenosis (late catch-up phenomenon)¹⁰ unless DCA and pathological examination were performed. According to the definitions of stent thrombosis by either previous clinical studies or the ARC,^{5–7} the thrombotic occlusion of SES in the present case is not defined as stent thrombosis because the patient did not present with ACS. Thus, the incidence of thrombotic occlusion of DES may be higher than reported. There were well-developed collaterals in the present case, which might have prevented the patient from presenting with ACS. A previous study showed that, utilizing a sensor-tipped pressure guidewire, one-fifth of individuals without stenotic lesions had immediately recruitable collateral flow to the respective vascular area sufficient to prevent myocardial ischemia during a brief coronary occlusion.¹¹ In the present case, before SES implantation, collateral vessels from the right coronary artery supplied the distal LAD, so there may have been rapid recruitment of well-developed collaterals.^{11,12} Gradual thrombus formation in SES, not resulting in sudden total occlusion, and recruitment of well-developed collaterals is another possibility for the patient not having presented with ACS. Silent thrombotic occlusion of a stent may occur in patients with no symptoms of myocardial ischemia (ie, some patients with diabetes mellitus or stent implantation in the infarct-related artery),¹³ although the present case had exertional angina and did not have diabetes mellitus or a history of previous myocardial infarction.

Conclusions

This case report shows very late thrombotic occlusion of

DES in a patient without ACS, which was confirmed by specimens extracted by DCA. The incidence of very late thrombotic occlusion of DES might be higher than reported.

References

1. Kitahara H, Kobayashi Y, Fujimoto Y, Nakamura Y, Nakayama T, Kuroda N, et al. Late stent thrombosis in patients receiving ticlopidine and aspirin after sirolimus-eluting stent implantation. *Circ J* 2008; **72**: 168–169.
2. Kuchulakanti PK, Chu WW, Torguson R, Ohlmann P, Rha SW, Clavijo LC, et al. Correlates and long-term outcomes of angiographically proven stent thrombosis with sirolimus- and paclitaxel-eluting stents. *Circulation* 2006; **113**: 1108–1113.
3. Iakovou I, Schmidt T, Bonizzoni E, Ge L, Sangiorgi GM, Stankovic G, et al. Incidence, predictors, and outcome of thrombosis after successful implantation of drug-eluting stents. *JAMA* 2005; **293**: 2126–2130.
4. Iwata Y, Kobayashi Y, Fukushima K, Kitahara H, Asano T, Ishio N, et al. Incidence of premature discontinuation of antiplatelet therapy after sirolimus-eluting stent implantation. *Circ J* 2008; **72**: 340–341.
5. Mauri L, Hsieh WH, Massaro JM, Ho KK, D'Agostino R, Cutlip DE. Stent thrombosis in randomized clinical trials of drug-eluting stents. *N Engl J Med* 2007; **356**: 1020–1029.
6. Moses JW, Leon MB, Popma JJ, Fitzgerald PJ, Holmes DR, O'Shaughnessy C, et al. Sirolimus-eluting stents versus standard stents in patients with stenosis in a native coronary artery. *N Engl J Med* 2003; **349**: 1315–1323.
7. Stone GW, Ellis SG, Cox DA, Hermiller J, O'Shaughnessy C, Mann JT, et al. A polymer-based, paclitaxel-eluting stent in patients with coronary artery disease. *N Engl J Med* 2004; **350**: 221–231.
8. Virmani R, Liistro F, Stankovic G, Di Mario C, Montorfano M, Farb A, et al. Mechanism of late in-stent restenosis after implantation of a paclitaxel derivate-eluting polymer stent system in humans. *Circulation* 2002; **106**: 2649–2651.
9. van Beusekom HM, Saia F, Zindler JD, Lemos PA, Swager-Ten Hoor SL, van Leeuwen MA, et al. Drug-eluting stents show delayed healing: Paclitaxel more pronounced than sirolimus. *Eur Heart J* 2007; **28**: 974–979.
10. Cosgrave J, Corbett SJ, Melzi G, Babic R, Biondi-Zoccai GG, Airolidi F, et al. Late restenosis following sirolimus-eluting stent implantation. *Am J Cardiol* 2007; **100**: 41–44.
11. Wustmann K, Zbinden S, Windecker S, Meier B, Seiler C. Is there functional collateral flow during vascular occlusion in angiographically normal coronary arteries? *Circulation* 2003; **107**: 2213–2220.
12. Perera D, Kanaganayagam GS, Saha M, Rashid R, Marber MS, Redwood SR. Coronary collaterals remain recruitable after percutaneous intervention. *Circulation* 2007; **115**: 2015–2021.
13. Xanthos T, Ekmektzoglou KA, Papadimitriou L. Reviewing myocardial silent ischemia: Specific patient subgroups. *Int J Cardiol* 2008; **124**: 139–148.



Sonic hedgehog is a critical mediator of erythropoietin-induced cardiac protection in mice

Kazutaka Ueda,¹ Hiroyuki Takano,¹ Yuriko Niitsuma,^{1,2} Hiroshi Hasegawa,¹ Raita Uchiyama,¹ Toru Oka,¹ Masaru Miyazaki,² Haruaki Nakaya,³ and Issei Komuro¹

¹Department of Cardiovascular Science and Medicine, ²Department of General Surgery, and ³Department of Pharmacology, Chiba University Graduate School of Medicine, Chiba, Japan.

Erythropoietin reportedly has beneficial effects on the heart after myocardial infarction, but the underlying mechanisms of these effects are unknown. We here demonstrate that sonic hedgehog is a critical mediator of erythropoietin-induced cardioprotection in mice. Treatment of mice with erythropoietin inhibited left ventricular remodeling and improved cardiac function after myocardial infarction, independent of erythropoiesis and the mobilization of bone marrow-derived cells. Erythropoietin prevented cardiomyocyte apoptosis and increased the number of capillaries and mature vessels in infarcted hearts by upregulating the expression of angiogenic cytokines such as VEGF and angiopoietin-1 in cardiomyocytes. Erythropoietin also increased the expression of sonic hedgehog in cardiomyocytes, and inhibition of sonic hedgehog signaling suppressed the erythropoietin-induced increase in angiogenic cytokine expression. Furthermore, the beneficial effects of erythropoietin on infarcted hearts were abolished by cardiomyocyte-specific deletion of sonic hedgehog. These results suggest that erythropoietin protects the heart after myocardial infarction by inducing angiogenesis through sonic hedgehog signaling.

Introduction

Recent medical advances have improved survival rates of patients with acute myocardial infarction (MI), whereas the number of patients showing heart failure after MI has increased in recent years (1). LV remodeling, which includes dilatation of the ventricle and increased interstitial fibrosis, is the critical process that underlies the progression to heart failure (1). Although pharmacological therapies are effective, heart failure is still one of the leading causes of death worldwide (2). It is thus important to elucidate a novel approach to prevent LV remodeling after MI.

Several hematopoietic cytokines including erythropoietin (EPO), G-CSF, and stem cell factor have been reported to prevent cardiac remodeling and dysfunction after MI in various animal models (3–5). EPO, a major regulator of erythroid progenitors, has attracted great attention because its administration induced significant improvements in the clinical status and LV function of patients with congestive heart failure (6, 7). Although several mechanisms of cardioprotective effects by EPO have been suggested, the precise mechanisms remain largely unknown (8–14). Treatment with EPO reverses the decreased oxygen-carrying capacity associated with anemia, which is often observed in patients with heart failure (8). EPO has also been reported to mobilize endothelial progenitor cells (EPCs) from bone marrow, leading to neovascularization in the heart (9). In addition, since EPO receptors (EPORs) are expressed in various types of cells including cardiomyocytes, EPO may have direct protective effects on cardiomyocytes (10–14).

In the present study, we investigated the mechanisms of how EPO induced cardioprotection after MI. We observed that EPO directly

prevented apoptotic death of cardiomyocytes and enhanced the expression of angiogenic cytokines, which induced robust angiogenesis, leading to the improvement of contractile function after MI. EPO also increased expression levels of sonic hedgehog (Shh) in cardiomyocytes, and the inhibition of Shh signaling abolished the EPO-induced increases of angiogenic cytokine production in cardiomyocytes. In hearts of cardiac-specific inducible Shh knockout (Shh-MerCre) mice, EPO treatment failed to upregulate angiogenic cytokines, enhance angiogenesis, and inhibit LV remodeling. Our results suggest that Shh is a key mediator of EPO-evoked cardioprotection in infarcted hearts.

Results

EPO prevents cardiac remodeling after MI. We subcutaneously administered EPO (10,000 U/kg/d) or saline immediately after coronary artery ligation until 4 days after MI. Fourteen days after MI, we histologically assessed the infarct size and examined cardiac function using echocardiography. Treatment with EPO significantly prevented enlargement of LV end-diastolic dimension (LVEDD) and reduction of fractional shortening (FS) and reduced the infarct size (fibrotic area/LV free wall) compared with saline treatment (Figure 1, A and B), suggesting that EPO prevents LV remodeling and dysfunction after MI.

The role of hematopoietic effects of EPO in cardioprotection (6, 7) was examined using transgene-rescued EPOR-null (RES) mice, which express EPORs only in the hematopoietic lineage (15). Although EPO treatment increased blood hemoglobin levels 7 days after MI in both WT and RES mice (Figure 2A), the cardioprotective effects of EPO were observed only in WT mice but not in the RES mice (Figure 1 and Figure 2B). EPO and saline did not show any significant differences in LVEDD, FS, or infarct size in the RES mice (Figure 2B), suggesting that erythropoiesis is not involved in the cardioprotective effects of EPO.

Authorship note: Kazutaka Ueda, Hiroyuki Takano, and Yuriko Niitsuma contributed equally to this work.

Conflict of interest: The authors have declared that no conflict of interest exists.

Citation for this article: *J Clin Invest* doi:10.1172/JCI39896.

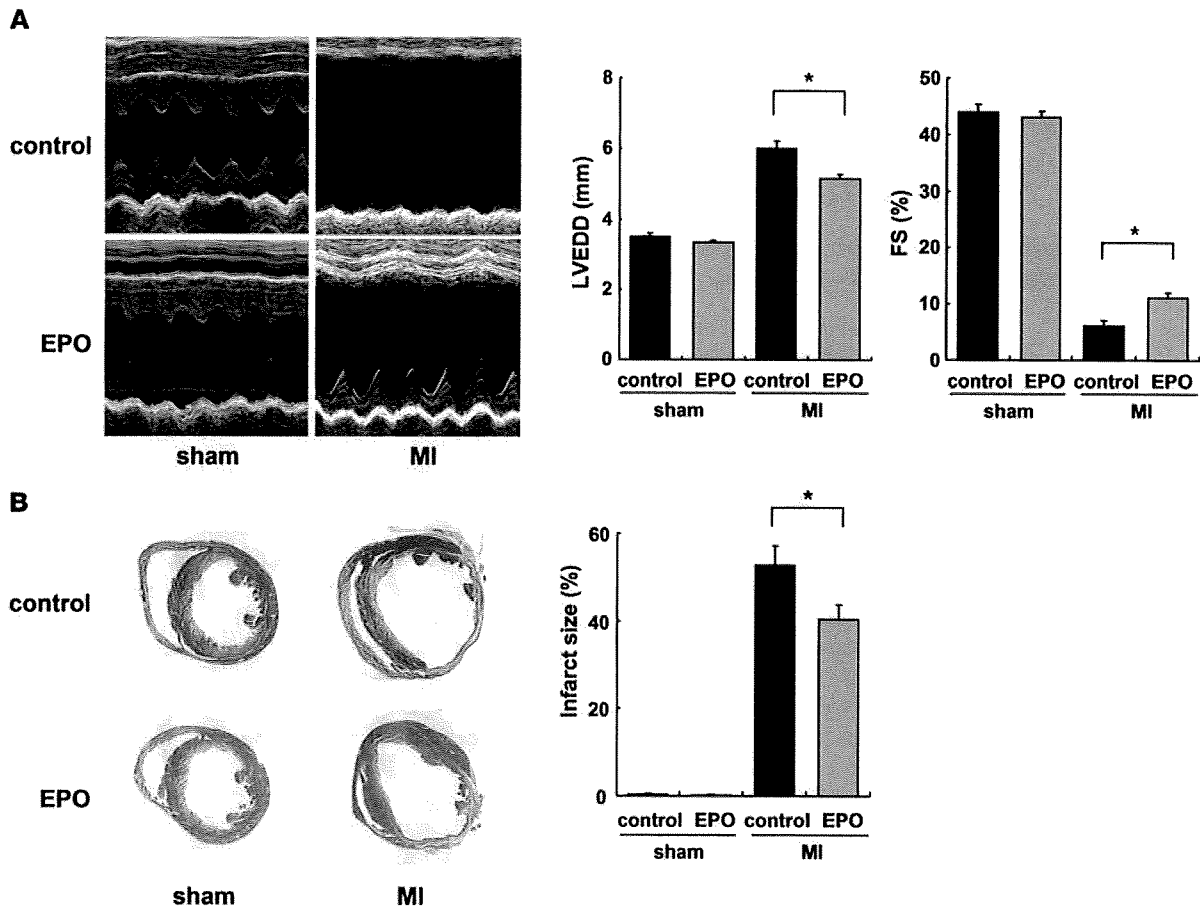


Figure 1 EPO prevents cardiac remodeling after MI. The effects of EPO treatment on LV function and infarct size were examined 14 days after operation. WT mice were subjected to MI or sham operation and treated with EPO or saline (control). (A) Echocardiographic analysis. ($n = 8-10$). (B) Masson trichrome staining of hearts and infarct size ($n = 8-10$). * $P < 0.01$.

To investigate whether EPO affects responses of inflammation and wound healing that may have an impact on LV remodeling after MI (16, 17), we examined macrophage infiltration and myofibroblast accumulation in the ischemic area after MI by immunohistochemical staining. The number of Mac3-positive macrophages was markedly decreased by EPO treatment 14 days after MI (Supplemental Figure 1A; supplemental material available with this article; doi:10.1172/JCI39896DS1). The number of α -SMA-positive myofibroblasts was significantly increased in EPO-treated hearts compared with saline-treated hearts (Supplemental Figure 1B).

We next determined whether EPO induced the mobilization of EPCs from bone marrow into peripheral blood using flow cytometry (9). After MI, EPO significantly increased the number of circulating CD34/Flk-1-double-positive EPCs in WT mice but not in the RES mice (Figure 2C). We produced MI in WT mice in which the bone marrow was replaced with cells derived from GFP-expressing mice. The hearts were excised 7 and 14 days after MI and immunohistochemically stained for PECAM. There were no differences in the number of GFP-positive cells and GFP/PECAM-double-positive cells in the border areas of EPO- and saline-treated infarcted hearts (Figure 2D), indicating that EPO did not enhance the homing of bone marrow-derived cells or increase the number of bone marrow-derived endothelial cells in the damaged hearts, although

EPO induced mobilization of EPCs from bone marrow into peripheral circulation. In addition, EPO did not improve cardiac function or increase the number of vessels in infarcted hearts even in RES mice transplanted with bone marrow of WT mice (Figure 2E). It is thus unlikely that the EPO-mobilized bone marrow-derived cells contribute to the cardioprotective effects of EPO.

EPO inhibits cardiomyocyte apoptosis in infarcted hearts. Apoptotic death of cardiomyocytes has been suggested to cause LV remodeling and dysfunction (18). To determine the role of antiapoptotic effects of EPO in cardioprotection, we performed TUNEL staining of hearts 24 hours after MI. The number of TUNEL-positive cardiomyocytes in the border area was significantly smaller in EPO-treated mice than in saline-treated mice, while EPO treatment had no effect on cardiomyocyte apoptosis in RES mice (Figure 3A). Western blot analysis showed that EPO treatment markedly reduced the level of cleaved caspase-3 in hearts at 24 hours after MI (Figure 3B). TUNEL staining revealed that pretreatment with EPO significantly attenuated H_2O_2 -induced apoptotic death in cultured cardiomyocytes of neonatal rats (Figure 3C). At 24 hours after exposing cardiomyocytes to H_2O_2 , expression levels of the antiapoptotic protein Bcl-2 were decreased, whereas levels of cleaved caspase-3 were increased, and these changes were inhibited markedly by EPO pretreatment (Figure 3D). Annexin V staining

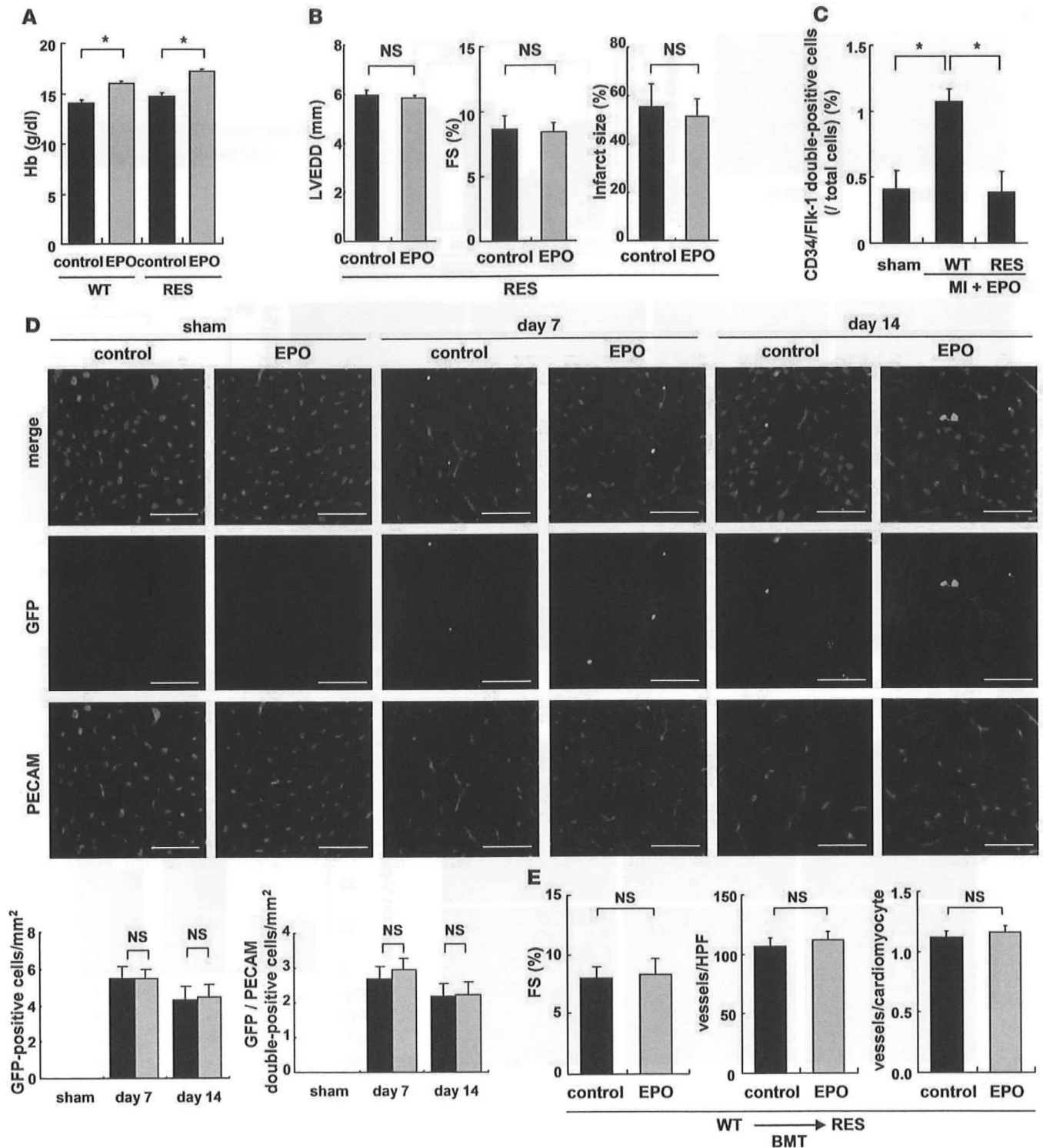


Figure 2

Erythroid hematogenesis is not required for the protective effects of EPO, and EPO does not accelerate the cardiac homing of bone marrow-derived cells after MI. WT and RES mice were subjected to MI and treated with EPO or saline (control). (A) Blood hemoglobin (Hb) levels 7 days after MI ($n = 4$). $*P < 0.01$. (B) Echocardiography and Masson trichrome staining were performed to analyze LV function and infarct size ($n = 10$). (C) Following MI and EPO treatment, the number of circulating CD34/Flk-1–double-positive EPCs increased in WT mice but not in RES mice. $*P < 0.05$ ($n = 4$). (D) Bone marrow cells from GFP-expressing mice were transplanted into WT mice. 7 and 14 days after MI, immunohistochemical staining for PECAM (red) was performed, and nuclei were counterstained with TO-PRO-3 (blue). GFP-positive cells (green) represent bone marrow–derived cells that moved into the heart and GFP/PECAM–double-positive cells denote bone marrow–derived endothelial cells. The numbers of GFP– and GFP/PECAM–double-positive cells in the border area (MI group) or LV free wall (sham group) were counted ($n = 5–8$). Scale bars: 50 μm. (E) WT bone marrow cells were transplanted (BMT) into RES mice, MI was induced, and the mice were treated with EPO or saline (control). FS, the number of vessels, and the ratio of vessels to cardiomyocytes in the border area are shown ($n = 8$).

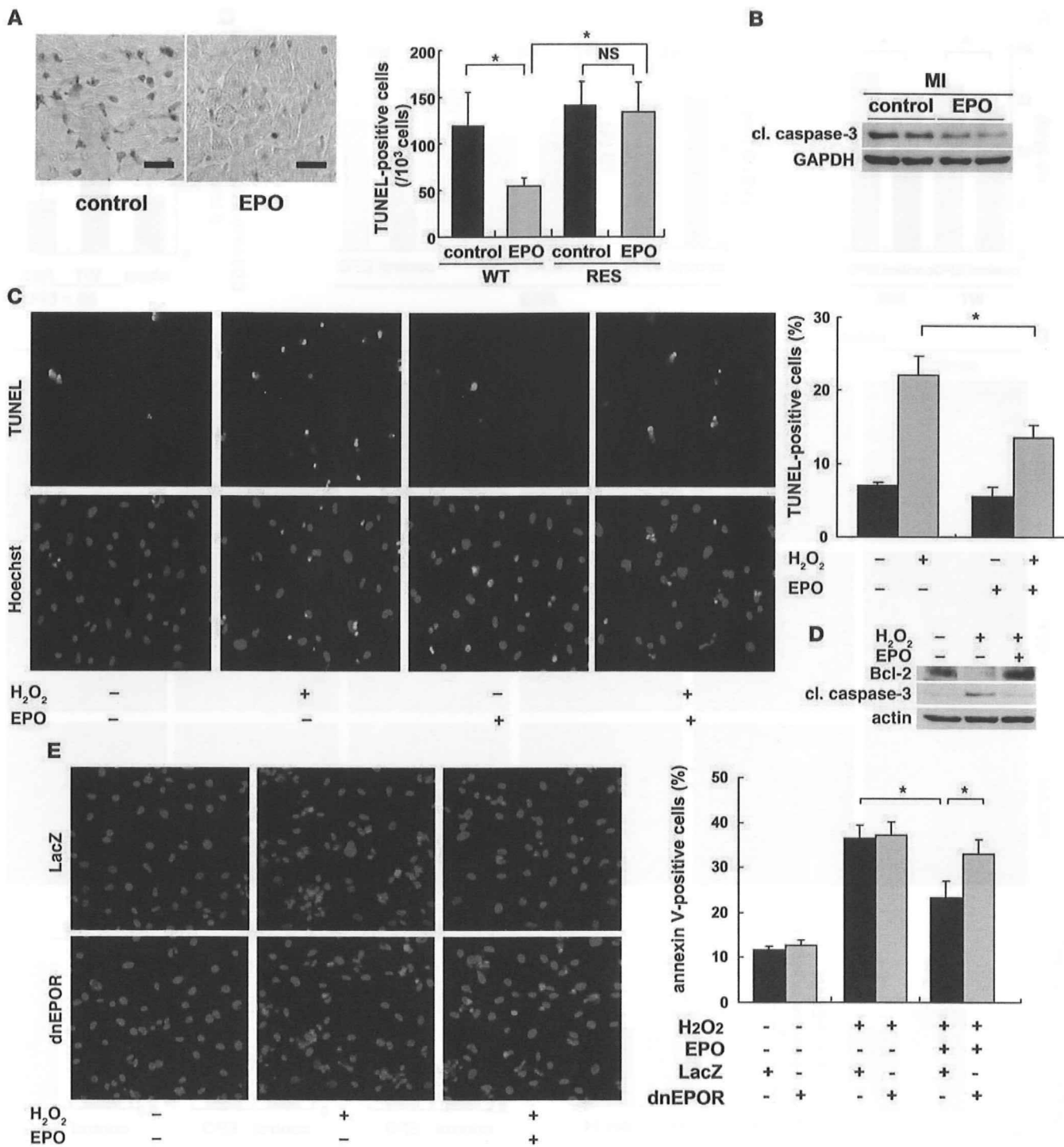
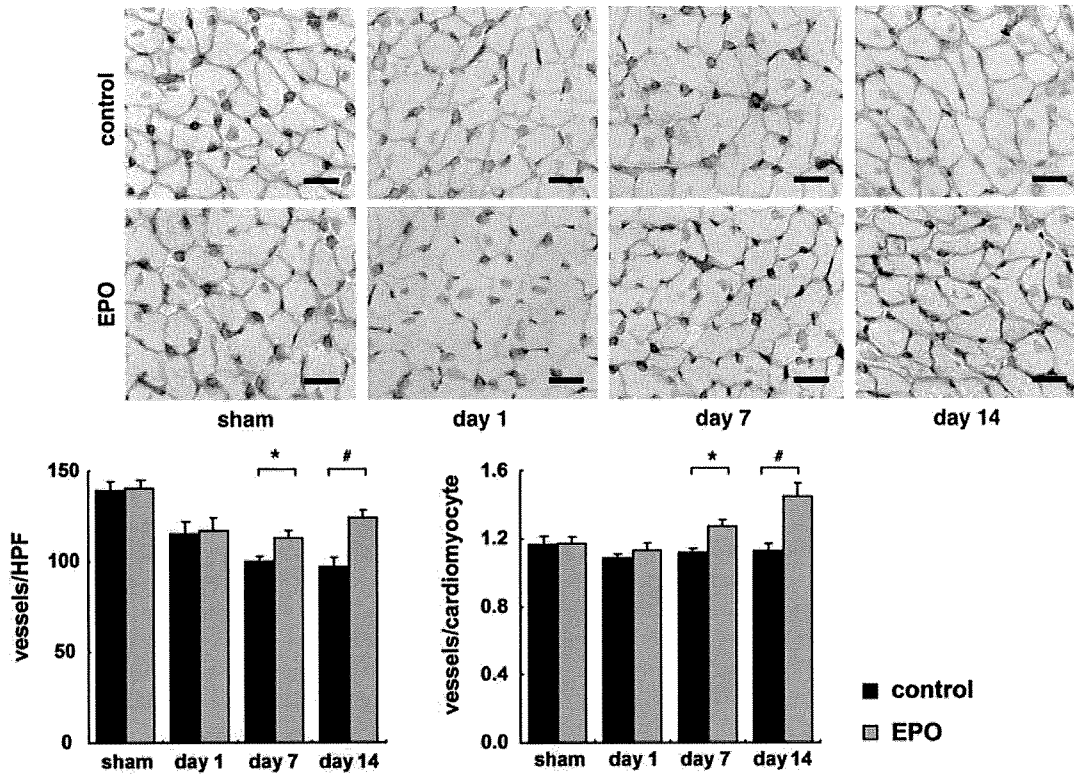


Figure 3

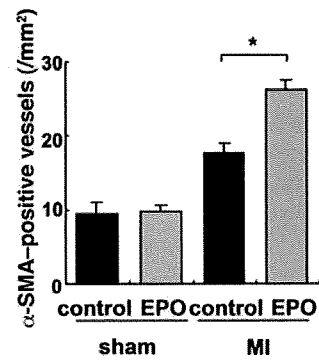
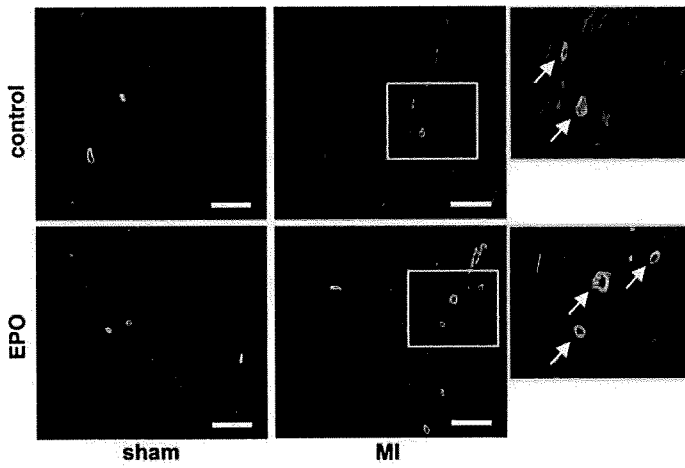
EPO inhibits cardiomyocyte apoptosis in infarcted hearts. (A) TUNEL staining (brown) of infarcted hearts from WT mice 24 hours after ligation. Scale bars: 100 μ m. The number of TUNEL-positive cardiomyocytes in the border area was counted. $*P < 0.01$ ($n = 10$). (B) Representative Western blots of cleaved caspase-3 (cl. caspase-3) protein in the heart 24 hours after MI are shown ($n = 4$). (C) Detection of apoptotic cardiomyocytes using FITC-labeled TUNEL staining (green). Nuclei were counterstained with Hoechst 33258 (blue). The TUNEL-positive cardiomyocytes were counted ($n = 10$). $*P < 0.05$. (D) Samples were pretreated with EPO for 8 hours before H₂O₂ treatment, and the expression of Bcl-2 and cleaved caspase-3 24 hours after H₂O₂ treatment was analyzed by Western blotting. Representative results from 3 experiments are shown. (E) Detection of apoptotic cardiomyocytes using Cy-3-labeled annexin V staining (red). Nuclei were counterstained with Hoechst 33258 (blue). Cardiomyocytes were infected with adenoviral vectors encoding dominant negative form of EPOR or LacZ at 10 MOI. The number of annexin V-positive cardiomyocytes was counted ($n = 10$). $*P < 0.05$.



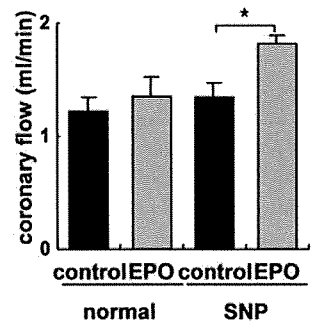
A



B



C



D

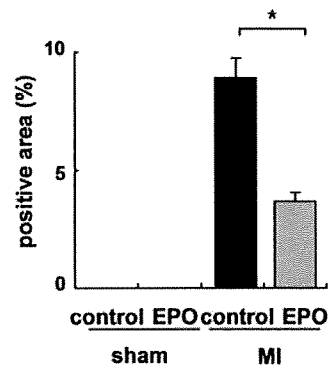
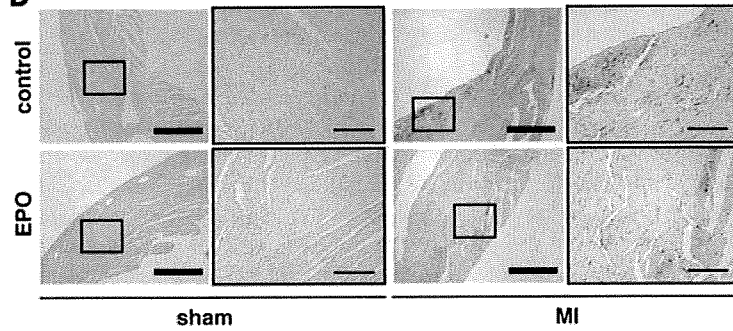




Figure 4

EPO promotes angiogenesis in infarcted hearts. (A) Double immunostaining for PECAM (green) and dystrophin (brown) in the border area (MI group) or LV free wall (sham group) of EPO- and saline-treated (control) hearts. Scale bars: 20 μm . The number of vessels and the ratio of vessels to cardiomyocyte were measured ($n = 8$ for each). * $P < 0.05$; # $P < 0.01$. (B) Double immunohistochemical staining for α SMA (green) and PECAM (red) shown together with TO-PRO-3 (blue) staining in the border area (MI group) or LV free wall (sham group) 14 days after operation. The number of α -SMA-positive vessels in the ischemic area was determined ($n = 8$). Scale bars: 100 μm . * $P < 0.05$. (C) Coronary flow was measured in EPO- and saline-treated (control) hearts 14 days after MI with or without sodium nitroprusside (SNP, 10^{-4} M) ($n = 6$). * $P < 0.05$. (D) Representative images of hypoxyprobe staining (brown) of EPO- and saline-treated (control) hearts in the border area (MI group) or LV free wall (sham group) 7 days after operation. The rate of hypoxyprobe-positive area in the border area was measured ($n = 3$). Scale bars: 500 μm (thick bars); 100 μm (thin bars). * $P < 0.01$.

showed that EPO-induced antiapoptotic effects were abolished by transducing adenoviral vectors, which encode the dominant negative form of EPOR (Figure 3E). These results suggest that EPO accomplishes antiapoptotic effects on cardiomyocytes through the EPO/EPOR signaling pathways. EPO has been reported to activate several kinases including Akt and ERK, which promote cell surviving pathways (10, 19). We thus determined whether EPO inhibits the death of cardiomyocytes by activating these kinases. Indeed, both Akt and ERK were activated in cultured cardiomyocytes by EPO in a time- and dose-dependent manner, and these activations were abolished by transducing dominant negative EPOR (Supplemental Figure 2, A–C). Inhibitions of Akt and ERK using respective kinase inhibitors suppressed EPO-induced reduction in the number of TUNEL-positive cardiomyocytes and EPO-induced downregulation of cleaved caspase-3 (Supplemental Figure 2, D and E), suggesting that EPO prevents apoptotic death of cardiomyocytes at least in part by activating Akt and ERK through the EPO/EPOR system in cardiomyocytes.

Angiogenic cytokines mediate EPO-induced cardioprotection. To determine the angiogenic effects of EPO, we performed immunohistochemical double-staining of infarcted hearts for PECAM and dystrophin. EPO treatment markedly increased the number of PECAM-positive capillary vessels and the ratio of vessels to cardiomyocytes in the border area at 7 days after MI (Figure 4A). Moreover, EPO significantly increased the number of α -SMA-positive vessels in the heart 14 days after MI (Figure 4B), suggesting that EPO induces the formation of mature vessels in infarcted hearts.

We also investigated the effects of EPO-induced angiogenesis on myocardial perfusion. At 14 days after MI, the coronary flow under dilatory stimulation with sodium nitroprusside was significantly increased in EPO-treated hearts compared with saline-treated hearts in the isolated heart perfusion system (Figure 4C). The extent of myocardial ischemia in the border area detected by Hypoxyprobe staining was decreased by EPO treatment (Figure 4D), suggesting that EPO-induced angiogenesis is functionally relevant to the enhancement of coronary perfusion reserve and the reduction of cardiac ischemia in infarcted hearts. Meanwhile, there were no significant differences in the cross-sectional area of cardiomyocytes in the border area at 14 days after MI between EPO and saline treatment (Supplemental Figure 3).

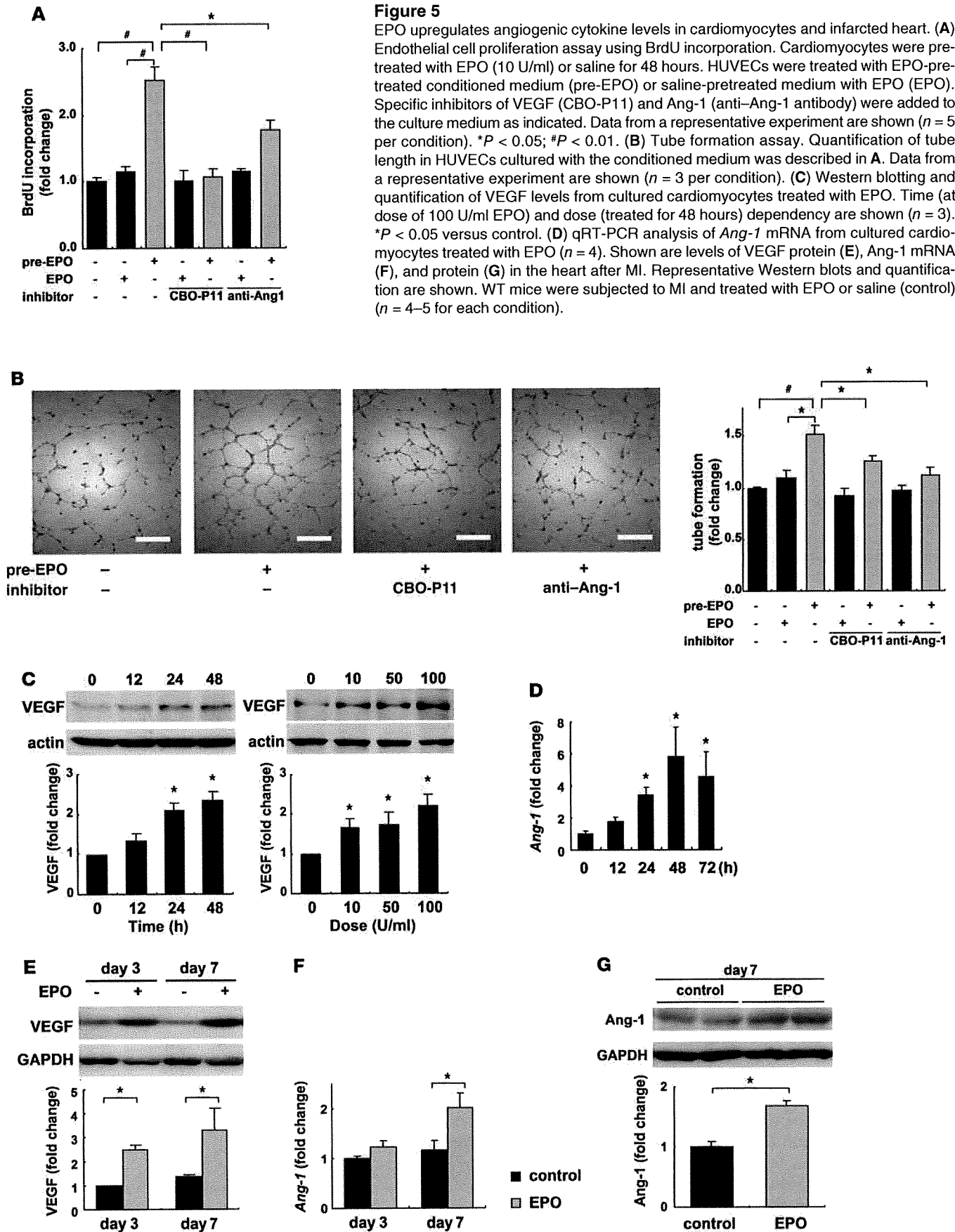
We also examined the mechanisms of EPO-induced angiogenesis in vitro using HUVECs. The administration of EPO did not increase BrdU incorporation into HUVECs. In contrast, the culture medium of cardiomyocytes conditioned by EPO markedly enhanced the BrdU incorporation into HUVECs compared with the cultured medium of cardiomyocytes conditioned by saline (Figure 5A). The conditioned medium from EPO-treated cardiomyocytes also significantly enhanced tube formation of HUVECs, whereas the administration of EPO itself did not affect tube formation of HUVECs cultured in the medium from saline-treated cardiomyocytes (Figure 5B). These results suggest that EPO evokes an angiogenic response by inducing paracrine factors secreted from cardiomyocytes.

EPO upregulated the levels of VEGF in cultured cardiomyocytes in both time- and dose-dependent manners (Figure 5C). EPO also upregulated the levels of angiopoietin-1 (*Ang-1*) mRNA in cardiomyocytes, as evidenced by quantitative RT-PCR (qRT-PCR) (Figure 5D). Proliferation and tube formation of HUVEC induced by the conditioned medium from EPO-treated cardiomyocytes were significantly suppressed by a VEGF-specific inhibitor (CBO-P11) or an anti-Ang-1 antibody (Figure 5, A and B). Additionally, when VEGF was knocked down in cardiomyocytes using siRNA, the EPO-induced proliferation of HUVECs was also suppressed (Supplemental Figure 4A). These results suggest that VEGF and Ang-1 secreted from cardiomyocytes mediate the EPO-induced angiogenic response.

Consistent with the in vitro results, EPO treatment markedly increased the levels of VEGF and Ang-1 proteins and *Ang-1* mRNA in the heart after MI (Figure 5, E–G). To determine the role of EPO-mediated VEGF expression in vivo, we injected an adenoviral vector encoding a soluble form of Flt-1, an inhibitor of VEGF, into the thigh muscles of WT mice 4 days before and 3 days after MI. The beneficial effects of EPO on infarcted hearts, including increased vessel number, reduced infarct size, and improved cardiac function, were all abolished by VEGF inhibition (Figure 6), suggesting that VEGF secreted from cardiomyocytes plays a critical role in the cardioprotective effects of EPO against MI.

Shh is a critical mediator of the angiogenic effects of EPO. We further investigated how EPO increases angiogenic cytokine levels in infarcted hearts. Since Akt and ERK, which are activated by EPO, have been reported to regulate VEGF expression (19, 20), we first determined whether EPO increased expression levels of VEGF by activating these kinases in cardiomyocytes. Although both Akt and ERK were activated by EPO in cultured cardiomyocytes, activation levels were not so high as compared with other growth factors such as insulin (Supplemental Figure 2B and data not shown). Since EPO-induced upregulation of VEGF was so robust, we hypothesized that other mitogens mediate the EPO-induced upregulation of VEGF. It has recently been reported that carbamylated EPO (CEPO) promotes neural progenitor cell proliferation and their differentiation into neurons through an upregulation of Shh expression (21). Shh, a critical regulator of patterning and growth in various tissues during embryogenesis, has been reported to show angiogenic effects in infarcted hearts (22, 23). We thus examined the involvement of Shh signaling in EPO-induced cardioprotection.

To determine whether EPO upregulates Shh expression in cardiomyocytes, we first examined the levels of Shh in cultured cardiomyocytes. Both EPO and CEPO induced a marked accumulation of the biologically active, aminoterminal fragment of Shh



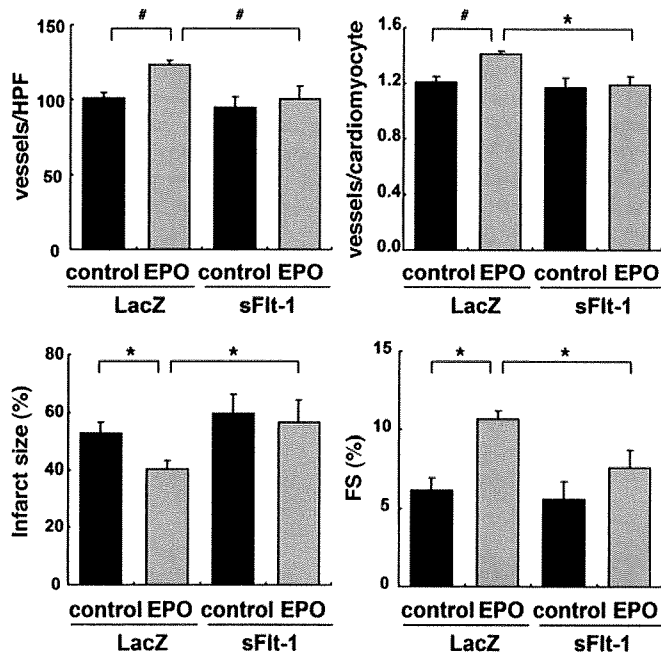


Figure 6
VEGF is essential for the angiogenic and cardioprotective effects of EPO. WT mice were injected with adenoviral vectors encoding soluble Flt-1 (sFlt-1) or LacZ, subjected to MI, and treated with EPO or saline (control). Echocardiographic analysis and immunohistochemical staining were then performed ($n = 8$). $*P < 0.05$; $\#P < 0.01$.

(Shh-N) in cardiomyocytes but not in cardiac fibroblasts 48 hours after treatment (Figure 7A), and Shh-N was abundantly secreted from EPO-treated cardiomyocytes into the culture medium (Figure 7B). Immunocytochemical analysis demonstrated that EPO induced the accumulation of Shh in α -sarcomeric actinin-positive cardiomyocytes but not in vimentin-positive cardiac fibroblasts (Figure 7C). In addition, EPO treatment significantly upregulated the levels of *Shh* mRNA in cardiomyocytes (Figure 7D).

We next determined whether Shh augmented angiogenic cytokine levels in cultured cardiomyocytes. Addition of recombinant murine Shh-N peptide (rmShh) increased the mRNA levels of the downstream target genes *Ptch1* and *Gli1* in cardiomyocytes in a dose-dependent manner (Figure 7E). rmShh also increased the levels of VEGF protein and *Ang-1* mRNA in cardiomyocytes as well as the concentration of VEGF protein in the culture medium (Figure 7, E and F). These changes were blocked by cyclopamine, a specific inhibitor of Shh signaling (Figure 7, E and F).

Cyclopamine treatment also significantly inhibited the EPO-induced increases in the levels of VEGF protein and *Ang-1* mRNA (Figure 8, A and B). Moreover, cyclopamine significantly inhibited the proliferation of HUVEC induced by conditioned medium from cardiomyocytes pretreated with EPO (Figure 8C). Consistently, knockdown of Shh in cardiomyocytes also inhibited the EPO-induced proliferation of HUVEC (Supplemental Figure 4B), indicating that EPO induces expression of angiogenic cytokines by activating Shh signaling in cardiomyocytes.

On the other hand, the EPO-induced inhibition of cardiomyocyte apoptosis 24 hours after exposure to H_2O_2 was not affected by cyclopamine (Figure 8D), suggesting that EPO shows its antiapoptotic effects on cardiomyocytes through a Shh-independent pathway.

Cardiomyocyte-specific Shh deletion abolishes EPO-induced cardioprotection. We next determined the role of Shh signaling in EPO-induced cardioprotection in vivo. The expression levels of Shh and Patched were increased in infarcted hearts (Figure 9A), as previously reported (23). Notably, expression levels of Shh and Patched protein were higher in infarcted hearts treated with EPO than in those treated with saline (Figure 9A), indicating that EPO activates Shh signaling in infarcted hearts. Meanwhile, there were no differences in the expression levels of Shh protein in the infarcted hearts of WT and RES mice, suggesting that endogenous EPO signaling is not associated with the upregulation of Shh in the infarcted hearts (Supplemental Figure 5).

Systemic deletion of Shh has been reported to result in cardiovascular defects in mice (24). To elucidate the roles of EPO-induced activation of Shh signaling pathways in infarcted hearts, we employed Shh-MerCre mice in which Shh is deleted only in cardiomyocytes following tamoxifen treatment. We crossed *Shh^{flxed/flxed}* mice (25) with the transgenic mice in which a transgene encoding Cre recombinase was fused to the mutated estrogen receptor domains (MerCreMer) driven by the cardiomyocyte specific α -myosin heavy chain (α -MHC) promoter (26), and then produced the MHC-MerCreMer; *Shh^{flxed/flxed}* mutant (Shh-MerCre) mice. After tamoxifen treatment, we confirmed that EPO-induced increases in the expression levels of Shh protein were significantly attenuated in the infarcted hearts of Shh-MerCre mice (Figure 9B). Under basal conditions at 7 days after tamoxifen treatment and at 14 days after MI, there were no significant differences in LV function or the number of vessels and the ratio of vessels to cardiomyocytes among Shh-MerCre mice, *Shh^{flxed/flxed}* mice, MHC-MerCreMer mice, and WT mice (Figure 9, C and D, and data not shown).

There were no significant differences in LVEDD, FS, and infarct size in the Shh-MerCre mice treated with or without EPO after MI (Figure 9C). EPO did not increase the number of vessels, the ratio of vessels to cardiomyocytes, and the number of α -SMA-positive vessels in Shh-MerCre mice (Figure 9D). EPO treatment also failed to upregulate VEGF protein and *Ang-1* mRNA levels in Shh-MerCre mice (Figure 9, E and F), suggesting that myocardial Shh signaling is critical for the angiogenic and cardioprotective effects of EPO in infarcted hearts.

The role of STAT3 in the mechanism of EPO-induced cardioprotection. We have recently reported that G-CSF prevents LV remodeling after MI through the JAK2/STAT3 pathway in cardiomyocytes (5). To determine whether STAT3 is also involved in cardioprotective effects of EPO, we produced an MI model in transgenic mice that express dominant negative STAT3 in cardiomyocytes under the control of the α -MHC promoter (dnSTAT3-Tg). In dnSTAT3-Tg mice, the EPO treatment reduced infarct size and ameliorated LV dysfunction and remodeling at 14 days after MI by the same degree as WT mice (Supplemental Figure 6A). Overexpression of dnSTAT3 had no effects on EPO-induced prevention of H_2O_2 -induced apoptotic death in cardiomyocytes (Supplemental Figure 6B), indicating that STAT3 is not involved in the mechanism of EPO-induced cardioprotective effects after MI.

Discussion

In the present study, we elucidated what we believe are novel mechanisms underlying the EPO-mediated inhibition of cardiac remodeling after MI. EPO enhanced the expression of angiogenic cytokines such as VEGF and *Ang-1* in cultured cardiomyocytes and infarcted hearts, which, in turn, induced the proliferation of vas-

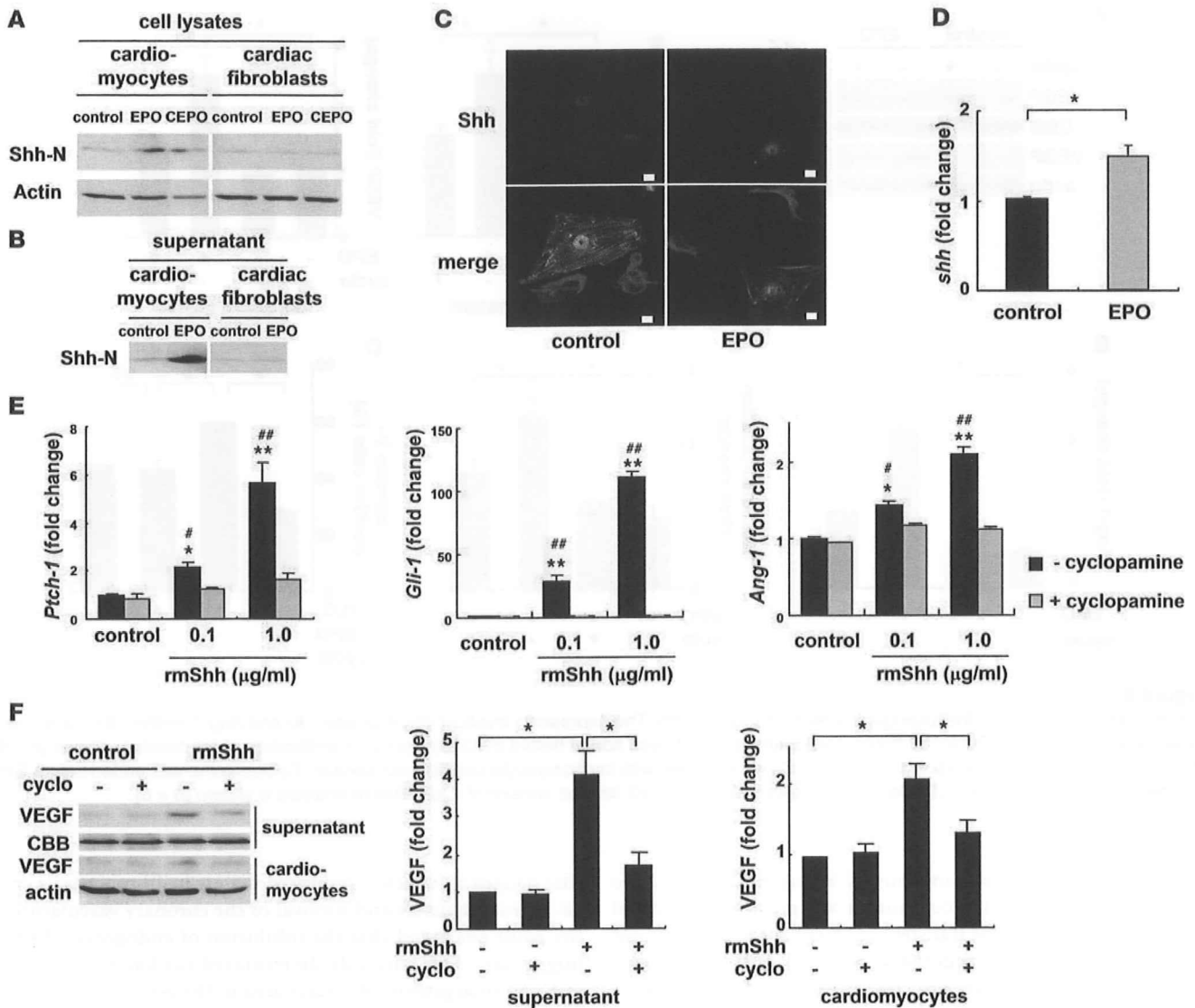


Figure 7

EPO upregulates expression levels of Shh. Western blotting of Shh in cultured neonatal rat cardiomyocytes and cardiac fibroblasts (A) and in the culture supernatants (B). Cells were treated with EPO (100 U/ml) or CEPO (100 U/ml) for 48 hours. Shh-N represents the aminoterminal domain of Shh, which is a biologically active form of Shh. (C) Immunocytochemical staining for Shh (red), α -sarcomeric actinin (green), and vimentin (blue). Cardiomyocytes and cardiac fibroblasts were cocultured with or without EPO for 48 hours. EPO induced the cytoplasmic accumulation of Shh in cardiomyocytes but not cardiac fibroblasts. Scale bars: 10 μ m. (D) qRT-PCR analysis of *Shh* mRNA. Cardiomyocytes were treated with EPO for 24 hours ($n = 5$). * $P < 0.05$. (E) qRT-PCR analysis of *Ptch-1*, *Gli-1*, and *Ang-1* mRNA. Cardiomyocytes were treated with rmShh (0.1 or 1.0 μ g/ml) for 24 hours ($n = 4$). * $P < 0.05$; ** $P < 0.01$ versus control. # $P < 0.05$; ## $P < 0.01$ versus rmShh and cyclopamine (5 μ M) treatment. (F) Western blotting of VEGF. Cardiomyocytes were treated with rmShh (1.0 μ g/ml) for 48 hours. Cyclopamine (cyclo) was administered 15 minutes before rmShh treatment. Representative Western blots and quantification of the bands are shown ($n = 4$).

cular endothelial cells and angiogenesis. EPO also increased Shh levels in cardiomyocytes, and the various effects evoked by EPO were attenuated by inhibiting Shh signaling (Figure 9G).

We found that EPO promoted angiogenesis by upregulating the expression of VEGF and Ang-1. VEGF is a key molecule that initiates proliferation and migration of endothelial cells and promotes the formation of new vessels, whereas chronic VEGF overexpression in mice has been reported to produce numerous small vessels lacking functional layers (27). Ang-1 induces recruitment of smooth muscle cells to primitive vessels consisting of endothelial cells (27–29). Therefore, our results suggest that EPO

treatment might be a better approach to creating stable and functional vessels in infarcted myocardium than the treatment with single angiogenic cytokine. Inhibition of angiogenesis by using the inhibitor of VEGF significantly attenuated the protective effects of EPO, such as the reduction of infarct size and improvement of LV function after MI. Since sufficient coronary perfusion resulting from angiogenesis can prevent cardiomyocyte apoptosis and improve contractile function (30, 31), angiogenic effects as well as direct antiapoptotic effects of EPO might protect the heart after MI. In this study, EPO did not enhance the homing of bone marrow-derived cells in damaged hearts, although EPO induced

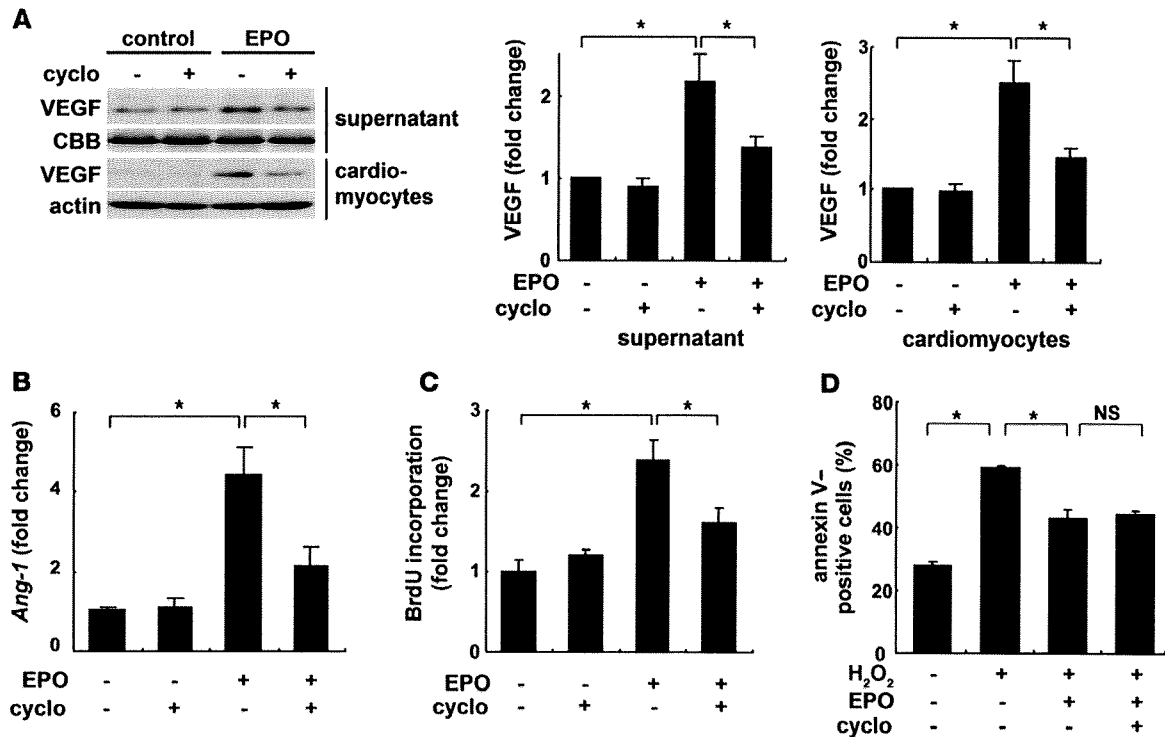


Figure 8

Shh is a critical mediator of the angiogenic effects of EPO in vitro. The expression levels of VEGF protein (A) and *Ang-1* mRNA (B). Cardiomyocytes were treated with EPO for 48 hours. Cyclopamine (5 μ M) was added before EPO treatment. Quantification of the bands is shown ($n = 4$). * $P < 0.05$. (C) HUVEC proliferation assay. HUVECs were treated with cardiomyocyte-conditioned medium. Cyclopamine was added before EPO treatment. $n = 5$ per condition. (D) Detection of apoptosis using Cy3-labeled annexin V. Quantitative analysis is shown ($n = 6$).

mobilization of bone marrow cells including EPCs from bone marrow into peripheral circulation. It was previously reported that intramyocardial gene transfer of Shh enhanced angiogenesis by bone marrow-derived endothelial cells (23). Although reasons for the different results are not clear at present, the discrepancy may come from expression levels of Shh. Expression levels of Shh produced by intramyocardial gene transfer might be much higher than those induced by subcutaneous injection of EPO, and mode of actions of Shh (i.e., autocrine, paracrine, and endocrine) may be dependent on the expression levels of Shh.

EPO upregulated expression of Shh in cardiomyocytes, which played a critical role in protection of the heart after MI by increasing angiogenic cytokine production. In infarcted hearts, expression levels of Shh and its downstream target Patched have been reported to be increased (23), and Shh has been shown to produce robust angiogenic effects (22, 23). A recent study has demonstrated that cardiomyocyte-specific deletion of *Smoothed*, an essential component of Shh signaling, reduces the expression of angiogenic genes and the number of coronary vessels, resulting in cardiomyocyte apoptosis and cardiac dysfunction, and that vascular smooth muscle cell-specific deletion of *Smoothed* does not affect angiogenesis and cardiac function (32). These results and observations suggest that Shh upregulated by EPO in cardiomyocytes acts on cardiomyocytes themselves in an autocrine manner and increases production of angiogenic cytokines. There were no significant differences in size and function of LV and infarct size among the Shh-MerCre mice, *Shh^{flxed/flxed}* mice, and MHC-MerCreMer mice without EPO after MI. It has been demonstrated

that hedgehog, which is produced mainly by fibroblasts, is critical for maintenance and survival of the coronary vasculature in the adult heart and that the inhibition of endogenous hedgehog by anti-Shh antibody deteriorated cardiac function and induced enlargement of infarct area in the post-MI hearts (32). The discrepancy may come from the different cells of Shh inhibition. Secretion of Shh from other cells including fibroblasts was not inhibited in the cardiomyocyte-specific Shh-deleted mice (Shh-MerCre mice). In neural stem cells, Shh expression is induced via the Notch receptor-mediated activation of cytoplasmic signaling molecules, including Akt, STAT3, and mammalian target of rapamycin (33). Furthermore, it has been also reported that *Shh* is a target gene of NF- κ B in mice (34). EPO is known to activate several signaling pathways, including Akt, STAT, and NF- κ B in various tissues (19, 35). Further studies are needed to clarify the signaling cascade by which EPO upregulates Shh expression in cardiomyocytes.

We previously demonstrated that angiogenesis promotes cardiac hypertrophy in mice during the early phase of pressure overload (30). We do not know why EPO did not induce cardiomyocyte hypertrophy in this study, but there is a possibility that MI itself induces cardiac and cardiomyocyte hypertrophy via increased wall stress, and EPO-induced reduction of infarct size might reduce the wall stress, resulting in prevention of cardiac and cardiomyocyte hypertrophy even with enhanced angiogenesis.

In conclusion, EPO prevented LV remodeling after MI through Shh. We have reported that G-CSF inhibits cardiomyocyte apoptosis by activating the JAK2/STAT3 pathway in cardio-

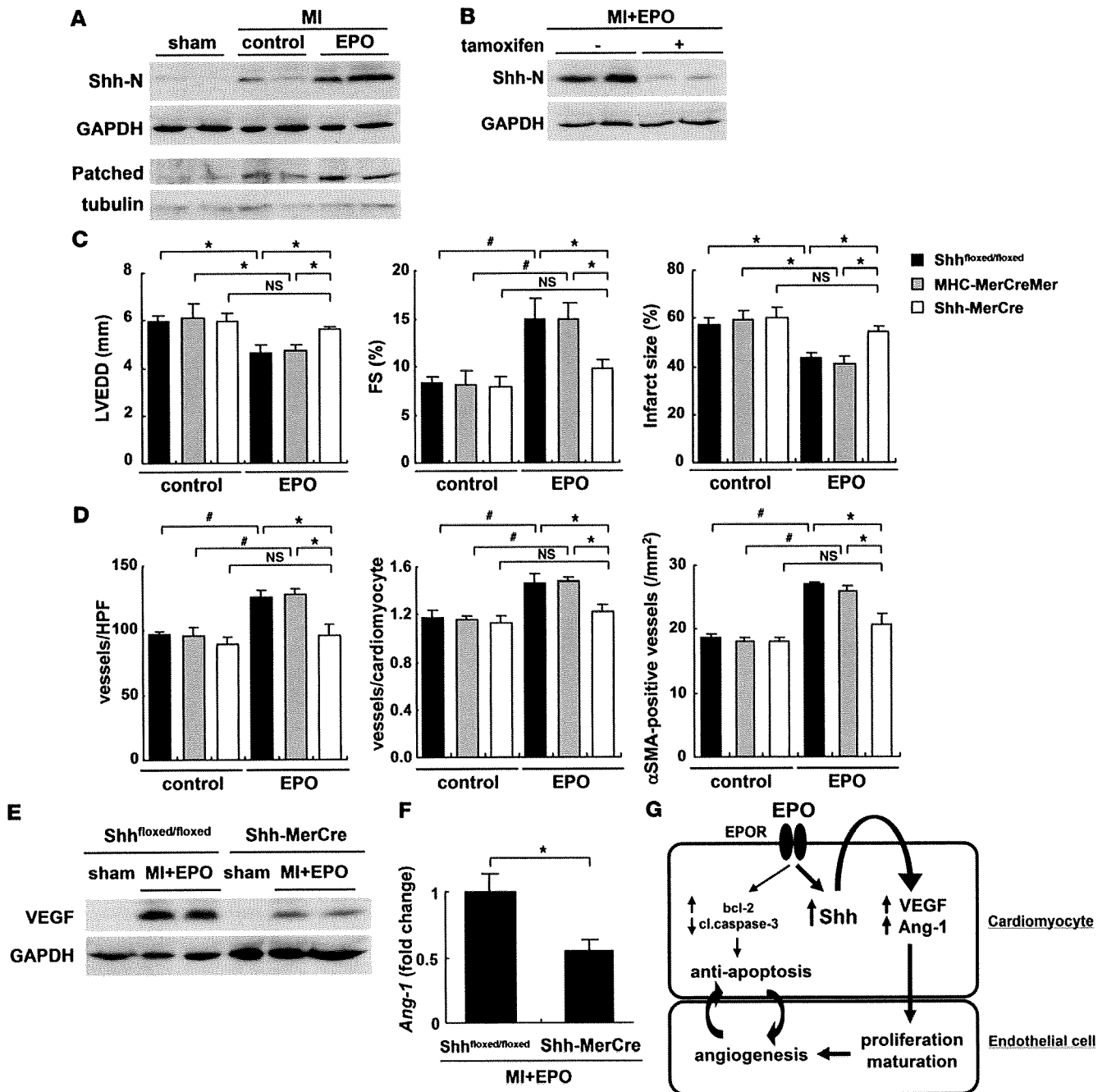


Figure 9

Cardiomyocyte-specific Shh deletion abolishes EPO-induced cardioprotection. (A) Activation of Shh signaling after MI and EPO treatment. Hearts were treated with EPO or saline (control) and harvested 4 days (for Shh-N) or 7 days (for Patched) after MI ($n = 4$ for each). (B) Western blotting of Shh-N in the infarcted hearts from Shh-MerCre mice treated with or without tamoxifen. Mice were subjected to MI, treated with EPO, and sacrificed 4 days after MI ($n = 4$ for each condition). We measured LVEDD, FS, infarct size (C), the number of vessels, the ratio of vessels to cardiomyocyte, and the number of α -SMA-positive vessels (D) 14 days after MI ($n = 8-14$). $*P < 0.05$; $\#P < 0.01$. (E and F) Western blotting of VEGF and qRT-PCR analysis of *Ang-1* mRNA in the heart 7 days after MI. All mice were treated with EPO ($n = 5$). $*P < 0.05$. (G) Proposed mechanism underlying the cardioprotective effects of EPO during MI. The mechanisms denoted by the thicker lines are thought to be particularly important.

myocytes, leading to reduced LV remodeling (5). EPO prevented cardiomyocyte apoptosis and protected the heart via the JAK2/STAT3-independent mechanisms, presenting the possibility that administration of the 2 cytokines synergistically protects the heart after MI.

Methods

Animals. All experimental procedures were performed according to the guidelines established by Chiba University for experiments in animals, and all protocols were approved by our institutional review board. Male (C57BL/6 background, 10- to 12-week-old) mice were used in this study.



research article

Shh^{flxed/flxed} mice were purchased from Jackson Laboratory. We injected each mouse with 8 mg/kg of tamoxifen (Sigma-Aldrich) for 12 consecutive days and produced MI at 7 days after tamoxifen treatment. Because EPOR-null mice are embryonic lethal due to severe anemia, we prepared RES mice expressing EPOR exclusively in the hematopoietic lineage, which were established as described previously (15). EPOR expression is limited to the erythroid lineage cells in the RES mice. The RES mice develop normally and are fertile. GFP transgenic mice were purchased from SLC. Generation and genotyping of dnSTAT3-Tg mice have been previously described (36). Age- and sex-matched WT mice (C57BL/6; SLC) were used as controls. RES mice were provided by M. Yamamoto (Tohoku University School of Medicine, Miyagi, Japan).

Induction of MI and treatment. Mice were anesthetized by intraperitoneal injection of pentobarbital (50 mg/kg) and artificially ventilated with a respirator. Mice were subjected to ligation of the left anterior descending artery or to sham operation as described previously (4). Sham operation was performed by cutting pericardium. EPO (Chugai Pharmaceutical) or the same volume of saline was administered subcutaneously.

Echocardiography. Transthoracic echocardiography was performed with a VisualSonics (Vevo 660; VisualSonics Inc.) equipped with a 25-MHz imaging transducer. Mice were kept awake without anesthesia during the echocardiographic examination to minimize data deviation, and heart rate was approximately 550–650 bpm in all mice.

Histology. Hearts fixed in 10% formalin were embedded in paraffin and sectioned at 4- μ m thickness for Masson trichrome staining. Tissue hypoxia was evaluated using the Hypoxyprobe (Chemicon) according to the manufacturer's instructions. Fixed frozen sections of the heart samples were immunohistochemically stained by using primary antibodies to PECAM (PharMingen), dystrophin (Novocastra Laboratories), α -SMA (DAKO), and Mac3 (BD Biosciences). The ischemic area that indicates infarct and border area was measured. For measurement of the cross-sectional area of cardiomyocytes, 50 randomly selected cardiomyocytes in a LV cross-section were measured by tracing dystrophin immunostaining. These measurements were performed with NIH ImageJ software. The samples were stained with Hoechst 33258 (1 μ g/ml) or TO-PRO-3 (Molecular Probes Inc.). Immunofluorescence was visualized by laser confocal microscopy (Radiance 2000; Bio-Rad Laboratories).

Bone marrow transplantation. Bone marrow cells were isolated from 8-week-old transgenic mice systemically expressing GFP or WT mice. Bone marrow cells (5×10^7 cells) suspended in 100 μ l of PBS containing 3% FBS were injected intravenously into irradiated WT mice or RES mice. A flow cytometric analysis revealed that more 97% of bone marrow cells were derived from donor cells at 6 weeks after bone marrow transplantation.

Flow cytometry. Circulating EPCs derived from bone marrow were detected by flow cytometry using CD34/Flk-1 double labeling. Mice subjected to MI or sham operation were treated with EPO or saline for 3 days subsequent to the operation. Then the mice were sacrificed to collect peripheral blood. The nucleated cells were incubated with FITC-conjugated anti-CD34 monoclonal antibody and PE-conjugated anti-Flk-1 antibody (VEGFR2/KDR; BD Biosciences) for 60 minutes on ice and washed with PBS supplemented with 3% FBS. The labeled nucleated cells were analyzed by the EPICS ALTRA flow cytometer using EXPO32 software (Beckman Coulter).

Western blot analysis. Western blot analysis was performed as described previously (30). Briefly, the infarcted hearts were separated into 2 parts consisting of the ischemic and viable regions. Proteins extracted from the ischemic regions of the infarcted hearts of mice were subjected to SDS-PAGE and then transferred onto polyvinylidene difluoride membranes (GE Healthcare). The membranes were probed using a primary antibody against, Shh-N (5E1; Developmental Studies Hybridoma Bank), VEGF, Patched, GAPDH (Santa Cruz Biotechnology Inc.), Ang-1 (Rockland), and α -tubulin (Sigma-Aldrich). For in vitro study, primary antibodies against Shh, Akt, Bcl-2

(Santa Cruz Biotechnology Inc.), VEGF for rat (R&D systems), phospho-Akt, phospho-ERK, cleaved caspase-3 (Cell Signaling), ERK (Invitrogen), and actin (Sigma-Aldrich) were used. The ECL-plus system (GE healthcare) was used for detection. Coomassie Brilliant Blue (Wako Pure Chemical Industries) was used for staining total protein blot with culture medium supernatant of cardiomyocytes.

In vivo gene transfer. Soluble Flt-1 is known to bind to VEGF, thereby acting on as an inhibitor for VEGF (37). We injected an adenoviral vector encoding the murine soluble *Flt-1* gene (10^9 pfu; Invitrogen) into thigh muscles of mice at 4 days before MI and 3 days after MI. Adenoviral vector encoding LacZ (10^9 PFU) was used as control.

Cell culture. Cardiomyocytes prepared from ventricles of 1-day-old Wistar rats were plated onto 35-mm plastic culture dishes at a concentration of 1×10^5 cells/cm² and cultured in DMEM supplemented with 10% FBS at 37°C in a mixture of 95% air and 5% CO₂. The culture medium was changed to serum-free DMEM 24 hours before stimulation. rmShh peptide was purchased from R&D Systems. The plasmid of a truncated form of human EPOR was from Y. Nakamura (RIKEN BioResource Center, Tsukuba, Ibaraki, Japan) (38). Adenoviral vector of truncated EPOR was created using AdEasy Vector System (Qbiogene). Adenoviral vector of dnSTAT3 was a gift from K. Yamauchi-Takahara (Osaka University, Osaka, Japan) (36). siRNA targeting VEGF, Shh, and negative control RNA (Invitrogen) were introduced into rat cardiomyocytes by using Lipofectamine RNAiMAX (Invitrogen) according to the manufacturer's instructions. For immunocytochemical staining, cardiomyocytes and cardiac fibroblasts were cocultured with or without EPO for 48 hours, fixed in 4% paraformaldehyde, and stained with primary antibodies to Shh (Santa Cruz Biotechnology Inc.), α -sarcomeric actinin (Sigma-Aldrich), and vimentin (Progen).

qRT-PCR. qRT-PCR analysis was performed as described previously (39). Total RNA was extracted from sample using the RNeasy kit (QIAGEN). We used 2.5 μ g of total RNA to generate cDNA using the Super Script VILO cDNA synthesis kit (Invitrogen). qRT-PCR was carried out on a LightCycler system (Roche) using probes from Universal Probe Library (Roche) and the TaqMan Master Mix (Roche). Sequence of primers and the respective Universal Probe Library probes were as follows: *Ang-1*: forward GGAAGATGGAAGCCTGGAT, reverse ACCAGAGGGATTCCCAAAC, probe #12; *Gapdh*: forward TGTCCTCGTGGATCTGAC, reverse CCT-GCTTACCACCTTCTTG, probe #80, each for mouse; *Shh*: forward GAATCCAAAGCTCGCATCC, reverse CAGGTGCACTGTGGCTGAT, probe #38; *Ang-1*: forward GGAAGCCTAGATTTCCAGAGG, reverse ACCAGAGGGATTCCCAAAC, probe #12; *Ptch-1*: forward CAAAGCT-GACTACATGCCAGA, reverse GCGTACTCTATGGGCTCTGC, probe #64; *Gli-1*: forward GGAAGAGAGCAGACTGACTGTG, reverse GGGGAGTG-GTCACTGCTG, probe #1; and *Gapdh*: forward AATGTATCCGTTGTG-GATCTGA, reverse GCTTACCACCTTCTTGATGT, probe #80, each for rat. Relative expression of target genes was calculated with the comparative CT method. Each sample was run in duplicate, and the results were systematically normalized using *Gapdh*.

Apoptosis analysis. Frozen sections of the heart samples and cultured cardiomyocytes fixed by 4% paraformaldehyde were subjected to TUNEL staining using a commercially available kit (In Situ Apoptosis Detection Kit; Takara Biomedicals) as directed by manufacturer. Annexin V-Cy3 Apoptosis Detection Kit (BioVision) was used to detect apoptotic cardiomyocytes according to the manufacturer's instructions. Cultured cardiomyocytes were serum starved in DMEM with 0.5% FBS and treated with EPO (10 U/ml) or normal saline for 8 hours prior to beginning H₂O₂ (100 μ M) treatment. Cyclopamine (40–42) (5 μ M), LY294002 (5 μ M), and PD98059 (10 μ M; Calbiochem) were administered 15 minutes before EPO treatment.



DNA synthesis assay. DNA synthesis was measured by performing a BrdU incorporation assay with a commercially available kit (Roche) as directed by the manufacturer. Cardiomyocyte-conditioned medium was collected as previously described (43). Briefly, cultured cardiomyocytes were starved in DMEM without FBS and were pretreated with EPO (10 U/ml) or saline for 48 hours, and then the medium was collected and transferred to HUVECs. HUVECs were plated in 96-well plates at a density of 5×10^4 cells/well in endothelial cell basal medium-2 with EGM-2 Bullet Kit (Cambrex) for 8 hours and then switched to cardiomyocyte-conditioned medium for 12 hours. BrdU was added to the medium, and BrdU incorporation was detected by ELISA using anti-BrdU antibody. VEGF receptor antagonist CBO-P11 (44, 45) ($12 \mu\text{M}$; Calbiochem) and anti-Ang-1 antibody ($1 \mu\text{g/ml}$; Chemicon) were used for the inhibition studies.

Tube formation assay. Matrigel (growth factor reduced, $100 \mu\text{l}$; BD Biosciences) was added to each well of a 48-well plate and allowed to polymerize at 37°C for 1 hour. HUVECs (1×10^4) were seeded onto Matrigel in endothelial cell basal medium-2 with EGM-2 Bullet Kit and cultured for 1 hour and then switched to cardiomyocyte-conditioned medium described above. After 8 hours, tube length was quantified using an angiogenesis image analyzer (Kurabo).

Isolated heart perfusion system. Isolated heart perfusion system was used to measure coronary flow as previously described (46). In brief, mouse hearts were excised rapidly and mounted on a Langendorff perfusion system. All isolated hearts were stabilized by perfusion of Krebs-Henseleit buffer, and perfusion pressure was adjusted to 60 mmHg. The heart was paced at 400 bpm. After an adjustment period, the coronary effluent was collected and the coronary flow was calculated. After baseline measure-

ments, sodium nitroprusside (10^{-4} M, Sigma-Aldrich) was infused into the perfusate, and coronary flow was measured.

Statistics. All data are shown as mean \pm SEM. Multiple group comparison was performed by 1-way ANOVA followed by Bonferroni's procedure for comparison of means. Comparison between 2 groups was analyzed by the 2-tailed Student's *t* test. Values of $P < 0.05$ were considered statistically significant.

Acknowledgments

The authors thank M. Yamamoto (Tohoku University School of Medicine, Miyagi, Japan) for generously providing RES mice. The authors thank Y. Ohtsuki, M. Ikeda, I. Sakamoto, A. Furuyama, M. Kikuchi, and H. Maruyama for their excellent technical assistance. This work was supported by a Grant-in-Aid for Scientific Research from the Ministry of Education, Science, Sports, and Culture, and Health and Labor Sciences research grants (to I. Komuro) and a Grant-in-Aid for Scientific Research from the Ministry of Education, Culture, Sports, Science and Technology of Japan and grants from the Terumo Life Science Foundation (to H. Takano).

Received for publication May 18, 2009, and accepted in revised form March 24, 2010.

Address correspondence to: Issei Komuro, Department of Cardiovascular Science and Medicine, Chiba University Graduate School of Medicine, 1-8-1 Inohana, Chuo-ku, Chiba 260-8670, Japan. Phone: 81.43.226.2097; Fax: 81.43.226.2557; E-mail: komuro-ky@umin.ac.jp.

- Jessup M, Brozena S. Heart failure. *N Engl J Med*. 2003;348(20):2007–2018.
- Rosamond W, et al. Heart disease and stroke statistics—2008 update: a report from the American Heart Association Statistics Committee and Stroke Statistics Subcommittee. *Circulation*. 2008;117(4):e25–146.
- Moon C, et al. Erythropoietin reduces myocardial infarction and left ventricular functional decline after coronary artery ligation in rats. *Proc Natl Acad Sci U S A*. 2003;100(20):11612–11617.
- Ohtsuka M, et al. Cytokine therapy prevents left ventricular remodeling and dysfunction after myocardial infarction through neovascularization. *FASEB J*. 2004;18(7):851–853.
- Harada M, et al. G-CSF prevents cardiac remodeling after myocardial infarction by activating the Jak-Stat pathway in cardiomyocytes. *Nat Med*. 2005;11(3):305–311.
- Silverberg DS, et al. The effect of correction of mild anemia in severe, resistant congestive heart failure using subcutaneous erythropoietin and intravenous iron: a randomized controlled study. *J Am Coll Cardiol*. 2001;37(7):1775–1780.
- Ponikowski P, et al. Effect of darbepoetin alfa on exercise tolerance in anemic patients with symptomatic chronic heart failure: a randomized, double-blind, placebo-controlled trial. *J Am Coll Cardiol*. 2007;49(7):753–762.
- Felker GM, Adams KF Jr, Gattis WA, O'Connor CM. Anemia as a risk factor and therapeutic target in heart failure. *J Am Coll Cardiol*. 2004;44(5):959–966.
- Bahlmann FH, et al. Erythropoietin regulates endothelial progenitor cells. *Blood*. 2004;103(3):921–926.
- Parsa C, et al. A novel protective effect of erythropoietin in the infarcted heart. *J Clin Invest*. 2003;112(7):999–1007.
- Wright GL, Hanlon P, Amin K, Steenbergen C, Murphy E, Arcasoy MO. Erythropoietin receptor expression in adult rat cardiomyocytes is associated with an acute cardioprotective effect for recombinant erythropoietin during ischemia-reperfusion injury. *FASEB J*. 2004;18(9):1031–1033.
- Brines M, Cerami A. Emerging biological roles for erythropoietin in the nervous system. *Nat Rev Neurosci*. 2005;6(6):484–494.
- Tada H, et al. Endogenous erythropoietin system in non-hematopoietic lineage cells plays a protective role in myocardial ischemia/reperfusion. *Cardiovasc Res*. 2006;71(3):466–477.
- Asaumi Y, et al. Protective role of endogenous erythropoietin system in nonhematopoietic cells against pressure overload-induced left ventricular dysfunction in mice. *Circulation*. 2007;115(15):2022–2032.
- Suzuki N, et al. Erythroid-specific expression of the erythropoietin receptor rescued its null mutant mice from lethality. *Blood*. 2002;100(7):2279–2288.
- Li Y, et al. Reduction of inflammatory cytokine expression and oxidative damage by erythropoietin in chronic heart failure. *Cardiovasc Res*. 2006;71(4):684–694.
- Hirose S, et al. Erythropoietin attenuates the development of experimental autoimmune myocarditis. *Cardiovasc Drugs Ther*. 2007;21(1):17–27.
- Abbate A, Biondi-Zoccai GG, Baldi A. Pathophysiologic role of myocardial apoptosis in post-infarction left ventricular remodeling. *J Cell Physiol*. 2002;193(2):145–153.
- Latini R, Brines M, Fiordaliso F. Do non-hemopoietic effects of erythropoietin play a beneficial role in heart failure? *Heart Fail Rev*. 2008;13(4):415–423.
- Pages G, Pouyssegur J. Transcriptional regulation of the Vascular Endothelial Growth Factor gene—a concert of activating factors. *Cardiovasc Res*. 2005;65(3):564–573.
- Wang L, et al. The sonic hedgehog pathway mediates carbamylated erythropoietin-enhanced proliferation and differentiation of adult neural progenitor cells. *J Biol Chem*. 2007;282(42):32462–32470.
- Pola R, et al. The morphogen sonic hedgehog is an indirect angiogenic agent upregulating two families of angiogenic growth factors. *Nat Med*. 2001;7(6):706–711.
- Kusano KF, et al. Sonic hedgehog myocardial gene therapy: tissue repair through transient reconstitution of embryonic signaling. *Nat Med*. 2005;11(11):1197–1204.
- Washington Smoak I, et al. Sonic hedgehog is required for cardiac outflow tract and neural crest cell development. *Dev Biol*. 2005;283(2):357–372.
- Lewis PM, et al. Cholesterol modification of sonic hedgehog is required for long-range signaling activity and effective modulation of signaling by Ptc1. *Cell*. 2001;105(5):599–612.
- Sohal DS, et al. Temporally regulated and tissue-specific gene manipulations in the adult and embryonic heart using a tamoxifen-inducible Cre protein. *Circ Res*. 2001;89(1):20–25.
- Suri C, et al. Increased vascularization in mice overexpressing angiopoietin-1. *Science*. 1998;282(5388):468–471.
- Asahara T, et al. Tie2 receptor ligands, angiopoietin-1 and angiopoietin-2, modulate VEGF-induced postnatal neovascularization. *Circ Res*. 1998;83(3):233–240.
- Holash J, Wiegand SJ, Yancopoulos GD. New model of tumor angiogenesis: dynamic balance between vessel regression and growth mediated by angiopoietins and VEGF. *Oncogene*. 1999;18(38):5356–5362.
- Sano M, et al. p53-induced inhibition of Hif-1 causes cardiac dysfunction during pressure overload. *Nature*. 2007;446(7134):444–448.
- Giordano FJ, et al. A cardiac myocyte vascular endothelial growth factor paracrine pathway is required to maintain cardiac function. *Proc Natl Acad Sci U S A*. 2001;98(10):5780–5785.
- Lavine KJ, Kovacs A, Ornitz DM. Hedgehog signaling is critical for maintenance of the adult coronary vasculature in mice. *J Clin Invest*. 2008;118(7):2404–2414.
- Androutsellis-Theotokis A, et al. Notch signaling regulates stem cell numbers in vitro and in vivo. *Nature*. 2006;442(7104):823–826.
- Kasperczyk H, Baumann B, Debatin KM, Fulda S. Characterization of sonic hedgehog as a novel



- NF-kappaB target gene that promotes NF-kappaB-mediated apoptosis resistance and tumor growth in vivo. *FASEB J.* 2009;23(1):21-33.
35. Digicaylioglu M, Lipton SA. Erythropoietin-mediated neuroprotection involves cross-talk between Jak2 and NF-kappaB signalling cascades. *Nature.* 2001;412(6847):641-647.
36. Funamoto M, et al. Signal transducer and activator of transcription 3 is required for glycoprotein 130-mediated induction of vascular endothelial growth factor in cardiac myocytes. *J Biol Chem.* 2000;275(14):10561-10566.
37. Kendall RL, Thomas KA. Inhibition of vascular endothelial cell growth factor activity by an endogenously encoded soluble receptor. *Proc Natl Acad Sci U S A.* 1993;90(22):10705-10709.
38. Nakamura Y, Komatsu N, Nakauchi H. A truncated erythropoietin receptor that fails to prevent programmed cell death of erythroid cells. *Science.* 1992;257(5073):1138-1141.
39. Leucht C, Stigloher C, Wizenmann A, Klafke R, Folchert A, Bally-Cuif L. MicroRNA-9 directs late organizer activity of the midbrain-hindbrain boundary. *Nat Neurosci.* 2008;11(6):641-648.
40. Taipale J, et al. Effects of oncogenic mutations in Smoothened and Patched can be reversed by cyclopamine. *Nature.* 2000;406(6799):1005-1009.
41. Berman D, et al. Medulloblastoma growth inhibition by hedgehog pathway blockade. *Science.* 2002;297(5586):1559-1561.
42. Watkins DN, Berman DM, Burkholder SG, Wang B, Beachy PA, Baylin SB. Hedgehog signalling within airway epithelial progenitors and in small-cell lung cancer. *Nature.* 2003;422(6929):313-317.
43. Zhang Y, Pasparakis M, Kollias G, Simons M. Myocyte-dependent regulation of endothelial cell syndecan-4 expression. Role of TNF-alpha. *J Biol Chem.* 1999;274(8):4786-4790.
44. Zilberberg L, et al. Structure and inhibitory effects on angiogenesis and tumor development of a new vascular endothelial growth inhibitor. *J Biol Chem.* 2003;278(37):35564-35573.
45. Heineke J, et al. Cardiomyocyte GATA4 functions as a stress-responsive regulator of angiogenesis in the murine heart. *J Clin Invest.* 2007;117(11):3198-3210.
46. Bendall J, et al. C. Strain-dependent variation in vascular responses to nitric oxide in the isolated murine heart. *J Mol Cell Cardiol.* 2002;34(10):1325-1333.

